Agricultural and Forest Meteorology 362 (2025) 110372

Contents lists available at ScienceDirect

Agricultural and Forest Meteorology

journal homepage: www.elsevier.com/locate/agrformet

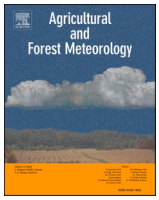

Increasing midday depression of mangrove photosynthesis with heat and drought stresses

Zhu Zhu [a,b,c,d], Xudong Zhu [a,b,c,d,e,f,*]

[a] State Key Laboratory of Marine Environmental Science, Xiamen University, Xiamen, Fujian, PR China
[b] National Observation and Research Station for the Taiwan Strait Marine Ecosystem (Xiamen University), Zhangzhou, Fujian, PR China
[c] Key Laboratory of the Coastal and Wetland Ecosystems (Ministry of Education), Xiamen University, Xiamen, Fujian, PR China
[d] College of the Environment and Ecology, Xiamen University, Xiamen, Fujian, PR China
[e] Shenzhen Research Institute of Xiamen University, Shenzhen, Guangdong, PR China
[f] Fujian Key Laboratory of Severe Weather, Fuzhou, Fujian, PR China

ARTICLE INFO

Keywords:
Gross primary productivity
Midday depression
Diurnal centroid
Eddy covariance
Environmental stresses

ABSTRACT

Midday depression of photosynthesis (MD) refers to the phenomenon that vegetation's photosynthetic rate decreases at midday experiencing environmental stresses. Mangrove MD and its responses to heat and drought stresses offer valuable insights into understanding the impact of climate change on mangrove blue carbon. However, the temporal variability of mangrove MD and its interactions with these stresses across short time scales remain less investigated. Here, we quantified mangrove MD using two diurnal metrics, relative midday depression (RMD) and diurnal centroid shift (DCS), and examined its responses to heat (air temperature) and drought (vapor pressure deficit (VPD) and rain) stresses in a subtropical estuarine wetland of Southeast China, based on six-year eddy covariance measurements from 2017 to 2022. The results indicate: (1) mangrove MD occurred at air temperature or VPD above a certain threshold but became severe when the stresses co-existed; (2) RMD performed better than DCS in measuring mangrove MD; (3) monthly RMD had a clear seasonal pattern peaking in summer (up to 26.1 %), while annual RMD (5.0 ~ 10.2 %) changed with gross primary productivity (GPP) in the opposite direction; (4) RMD increased with both air temperature (1.01 ~ 1.35 %/ °C) and VPD (8.41 ~ 13.79 %/kPa) for each year but with different sensitivities; (5) larger annual sensitivities of RMD to both air temperature and VPD tended to occur in drier years with less rain. This study highlights the importance of heat and drought stresses in affecting mangrove MD and GPP, implying that future warmer and drier climates are likely to weaken mangrove carbon uptake. Future empirical and model studies on mangrove blue carbon should explicitly consider sub-daily interactions between mangrove MD and environmental stresses to reduce the uncertainty in assessing mangrove carbon budget in the context of climate change.

1. Introduction

Mangroves are one of the coastal blue carbon ecosystems providing numerous important ecosystem services, such as carbon sequestration, coastal stabilization, and biodiversity maintenance (Alongi, 2014; Macreadie et al., 2021; Nellemann and Corcoran, 2009). Mangroves are highly productive and sequestrate 10 ~ 15 % of global coastal sediment carbon with only 0.5 % of the coastal area (Alongi, 2014). However, located in harsh habitats across the land-ocean interface, mangroves are more vulnerable to climate change and its consequences than terrestrial ecosystems (Alongi and Mukhopadhyay, 2015; Gou et al., 2023; Sharma et al., 2020). Notably, mangrove photosynthetic uptake rates of carbon dioxide (CO_2) are highly sensitive to various environmental stresses (Xia et al., 2015), such as high temperature (Chung et al., 2023), atmospheric drought (Sobrado, 1999), and high salinity (Lovelock et al., 2016). These heat and drought stresses and their impacts on mangrove photosynthesis are likely further amplified by future climate changes with increased temperature, enhanced vapor pressure deficit (VPD), and changing rainfall patterns (Myhre et al., 2019; Yuan et al., 2019). Thus, investigating the impact of heat and drought stresses on mangrove photosynthesis can help better understand the resilience and vulnerability of mangroves to climate change.

The temporal variability of vegetation photosynthesis across time scales offers valuable insights into the impacts of environmental stresses

* Corresponding author: Xiamen University, South Xiang'an Road, Xiamen, Fujian, China 361102.
E-mail address: xdzhu@xmu.edu.cn (X. Zhu).

https://doi.org/10.1016/j.agrformet.2024.110372
Received 11 April 2024; Received in revised form 2 December 2024; Accepted 13 December 2024

on gross primary productivity (GPP) (Li et al., 2023). The variability of GPP at longer time scales (e.g., seasonal and annual) is more regulated by phenology, climate, and disturbances, while the variability at shorter scales (e.g., diurnal) is mainly affected by meteorological factors such as light, temperature, and VPD. Diurnal variability of GPP can better reflect direct interactions between photosynthesis and environmental factors since these instantaneous interactions are likely obscured when interpreting the seasonal or annual variability of GPP using aggregating daily or multi-day observations (Xiao et al., 2021; Zhang et al., 2018). Midday depression of photosynthesis (MD) refers to the phenomenon that vegetation's photosynthetic rate decreases at midday when experiencing environmental stresses (Pons and Welschen, 2003; Xu and Shen, 1996). Given that heat and drought stresses, under which MD is usually observed, are also key characteristics of climate change, the interactions between MD and these stresses could serve as a proxy to assess the impacts of future climate change on vegetation photosynthesis (Li et al., 2023; Xiao et al., 2021).

The impacts of heat and drought stress on mangroves have been widely reported by previous studies covering growth dynamics (Duke et al., 2017; Prihantono et al., 2022; Zani et al., 2020) and carbon fluxes (Rodda et al., 2022; Sobrado, 1999; Tüffers et al., 1999; Zhu et al., 2021b). For example, both increasing temperature and VPD were found to suppress mangrove carbon uptake (Rodda et al., 2022; Zhu et al., 2021b). Rain was found to exert a delayed effect on mangrove greenness, peaking three months after high rainfall (Prihantono et al., 2022). Sobrado (1999) examined the drought effects on mangrove photosynthesis and observed a strong MD under contrasting salinities during both wet and dry seasons. Tüffers et al. (1999) also found significant MD in photosynthetic electron transport rates for sun-exposed leaves of two mangrove species. Although the key environmental controls have been identified by previous studies, we still have a limited understanding of how these environmental stresses affect mangrove MD quantitatively across time scales. The lack of high-frequency and long-term measurements of mangrove carbon fluxes is one of the major obstacles to prevent us from closing these knowledge gaps.

On the one hand, due to the limited availability of high-frequency carbon flux measurements in mangroves, few studies are exploring how mangrove MD respond to heat and drought stresses at a short diurnal scale. Wilson et al. (2003) proposed a 'diurnal centroid' method to discern whether the diurnal peak of carbon fluxes is weighted more towards the morning or afternoon, based on eddy covariance (EC) high-frequency flux measurements. Nelson et al. (2018) also applied the diurnal centroid approach to examine the drought response of the diurnal pattern of EC carbon fluxes. These studies on the diurnal pattern of carbon fluxes yielded much insight into MD, but their analyses mainly covered various types of terrestrial ecosystems. On the other hand, due to the lack of long-term carbon flux measurements, we also know little about the inter-annual variability of the responding sensitivity of mangrove MD to environmental stresses. Given that mangrove canopy height is highly dependent on salinity-related factors (Perri et al., 2023; Simard et al., 2019), the inter-annual variability of rain could also play an important role in regulating the response of mangrove MD to environmental stresses.

The application of the EC approach makes it possible to quantify net CO_2 exchange between ecosystem and the atmosphere (NEE) in a quasi-continuous manner (Baldocchi et al., 2001). Long-term and high-frequency flux time series serve as an ideal data source for examining the interactions between flux and environmental stresses across various time scales. Although the EC approach has been often applied in mangroves (Barr et al., 2010; Chen et al., 2023; Lu and Zhu, 2021; Rodda et al., 2022; Wang et al., 2023), we are not aware of any study to quantitatively assess mangrove MD using multi-year EC data. Our previous study has identified the occurrence of mangrove MD (Zhu et al., 2021a), but it is based on one-year EC data without explicitly quantitative assessment of mangrove MD and its responses to environmental stresses across time scales. In this study, we aim to conduct a thorough analysis of mangrove MD using six-year EC measurements from 2017 to 2022 in a subtropical estuarine wetland of Southeast China. The specific objectives are (1) to quantify temporal variations in mangrove MD across time scales, (2) to examine the response of mangrove MD to heat and drought stresses, and (3) to explore the inter-annual variation in the sensitivity of mangrove MD to environmental stresses. We hypothesize that (1) mangrove MD enhances with increasing heat and drought stresses, and (2) the sensitivity of mangrove MD to heat and drought stresses reduces with more rain.

2. Materials and methods

2.1. Study area

The study area is located in the Zhangjiang estuarine wetland of Southeast China, with a mangrove flux tower (23.92° N, 117.41°E) established as part of ChinaFLUX and USCCC networks (Fig. 1). Mangrove forests around the tower are mainly comprised of three mangrove species dominated by *Kandelia obovate*. These mangroves are inundated twice a day with a mean tidal range of 2.1 m and surface water salinity of 12.6 PSU and experience a monsoon climate with a mean air temperature of 21.1 °C and mean annual rain of 1165.5 mm (Lu and Zhu, 2021; Zhu et al., 2021b). The rain is seasonally uneven with the majority in spring and summer. All the field permits were acquired from Zhangjiang Estuary Mangrove National Nature Reserve, China. More details on the study area can be found in our previous studies (Lu and Zhu, 2021; 2021a; Zhu et al., 2019).

2.2. Eddy covariance and auxiliary measurements

Six-year continuous flux measurements from 2017 to 2022 were acquired using an EC system, comprised of a three-axis sonic anemometer (CSAT-3, Campbell Scientific, Inc., Logan, UT, USA) and an open path infrared gas analyzer (LI-7500, Li-COR Inc., Lincoln, NE, USA). Raw EC data were first recorded at 10 Hz and then processed into a 30-min time series of NEE after a series of flux calculations, corrections, and quality controls (Zhu et al., 2021b, 2021d), implemented in EddyPro6.1 software (Li-COR Inc., Lincoln, NE, USA). Auxiliary meteorological and tidal data used in this study include photosynthetically active radiation (PAR), air temperature (T_{air}), VPD, rain, and tidal inundation. PAR was measured by the PQS1 PAR Quantum sensor (Kipp & Zonen, Delft, The Netherlands) above the canopy. T_{air} and VPD were derived from the measurements by the HMP155A sensor (Vaisala, Helsinki, Finland) above the canopy. Rain was measured by the TE525 MM Rain Gage (Campbell Scientific, Inc., Logan, UT, USA) on the top of the flux tower. Tidal surface water level was derived from the measurements by HOBO U20L-04 Water Level Logger (Onset, Bourne, MA, USA) deployed above the sediment surface near the flux tower. Meteorological and tidal data were recorded at finer temporal resolutions but converted into a 30-minute time series for better comparisons with the flux data. In this study, 30-min mangrove GPP was calculated as the difference between estimated ecosystem respiration (*Re*) and observed NEE during the daytime, where a positive value indicated a downward atmosphere-mangrove CO_2 flux. Here, 30-min daytime *Re* was estimated from daytime air temperature using the temperature-respiration exponential equation fitted from 30-min nighttime measurements of air temperature and NEE without experiencing tidal inundation (Barr et al., 2013; Zhu et al., 2021d).

2.3. Relative midday depression and diurnal centroid shift

Similar to Xu and Shen (1996), the diurnal variations of mangrove GPP under various stress conditions can be divided into three typical patterns. The first is one-peaked experiencing no MD (represented by curve 1 in Fig. 1c), where GPP increases gradually in the morning, reaches its maximum around noon, and then decreases gradually in the

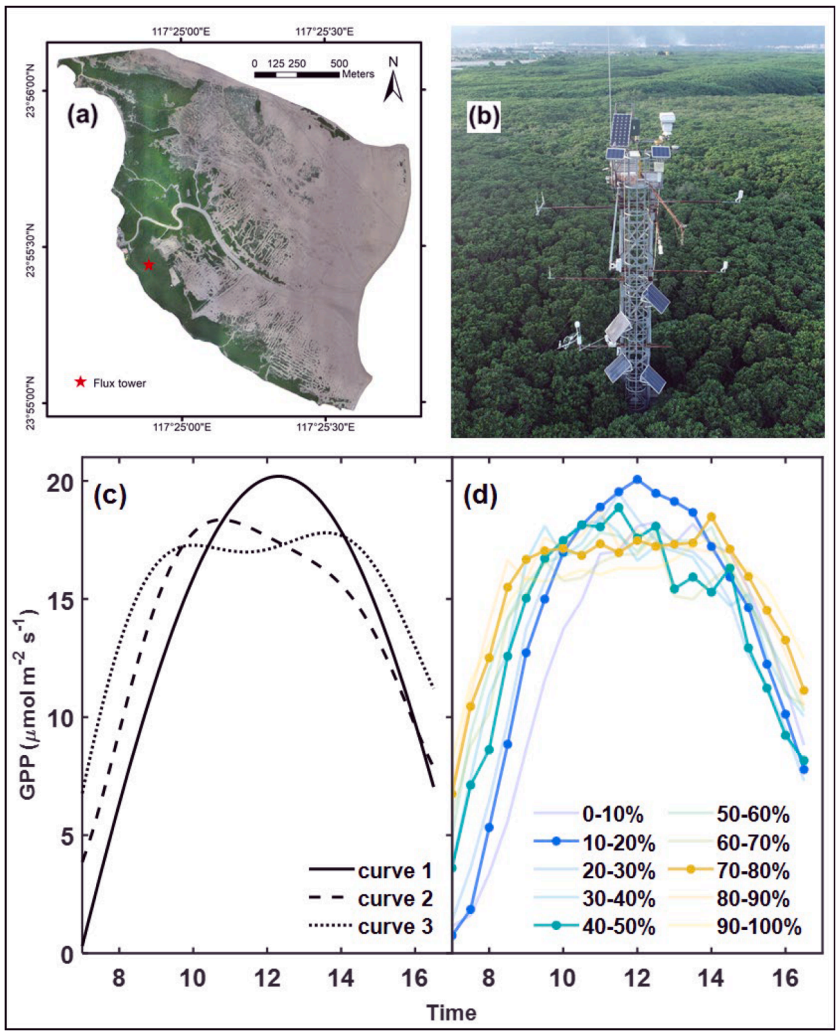

Fig. 1. Location of the study area (a) and mangrove eddy covariance (EC) flux tower (b) with three representative diurnal variation curves of gross primary productivity (GPP) (c). Each curve is fitted from the mean diurnal variation of 30-min EC-based GPP for the days within one joint tenth group (d), where curves 1, 2, and 3 correspond to the 2nd, 5th, and 8th joint tenth group, respectively. Each joint tenth group contains the days only when midday mean air temperature and VPD belong to the same tenth group.

afternoon. The second is also one-peaked experiencing moderate MD, with the peak shifting towards morning (curve 2). The third is two-peaked experiencing serious MD, with one peak in the morning and another in the afternoon (curve 3). To explore the MD quantitatively, for every single day, we fitted an 'ideal' parabola using 30-min GPP during daytime (7am ~ 5pm) excluding noon hours (10am ~ 2pm), and then calculated the MD of the day as the integrated difference in GPP between the fitted parabola (GPP_i) and actual diurnal course (GPP_a) over the noon hours. Given that GPP is time-dependent on light intensity or plant phenology, in this study we used the relative midday depression to noon-hour GPP_a (RMD, %) as a metric to quantify the severity of mangrove MD.

$$GPP_i(t) = a \times (t-b)^2 + c \tag{1}$$

where a, b, and c are fitting parameters with b indicating the time (t) of peak GPP.

$$RMD = \frac{\sum_{t_{n\_s}}^{t_{n\_e}} (GPP_i(t) - GPP_a(t))}{\sum_{t_{n\_s}}^{t_{n\_e}} GPP_a(t)} \times 100 \tag{2}$$

where t_{n_s} and t_{n_e} denote the start and end of noon hours (i.e., 10am and 2pm), respectively.

As the diurnal centroid method was often used in previous studies examining the response of carbon fluxes to heat or drought stress (Li et al., 2023; Nelson et al., 2018; Wilson et al., 2003), we also applied this metric to mangrove GPP in our analyses. Specifically, the diurnal centroid shift (DCS) between mangrove GPP and PAR was calculated as the difference in weighted mean hours of their diurnal courses (Wilson et al., 2003).

$$DCS = C_{GPP} - C_{PAR} = \frac{\sum_{t_{d\_s}}^{t_{d\_e}} (GPP_a(t) \times t)}{\sum_{t_{d\_s}}^{t_{d\_e}} GPP_a(t)} - \frac{\sum_{t_{d\_s}}^{t_{d\_e}} (PAR(t) \times t)}{\sum_{t_{d\_s}}^{t_{d\_e}} PAR(t)} \tag{3}$$

where t_{d_s} and t_{d_e} denote the start and end of daytime hours (i.e., 7 am and 5 pm), respectively; C_{GPP} and C_{PAR} denote the diurnal centroid of GPP and PAR, respectively. For example, if the diurnal course of GPP is perfectly symmetrical about noon, C_{GPP} would be 12 h. If GPP is greater in the morning, C_{GPP} would be <12 h. Here, the confounding effect due to the astronomical seasonal shift in PAR around local noon can be removed by the use of C_{PAR} as a reference. Thus, a negative DCS indicated a morning shift in the diurnal course of mangrove GPP, while a positive value indicated an afternoon shift.

2.4. Statistical analyses

In this study, missing gaps in 30-min time series were not gap-filled

to avoid assuming a priori relationships between carbon flux and environmental variables (Wilson et al., 2003). Any days with valid 30-min daytime data of less than half were excluded in the calculations of two diurnal metrics (i.e., RMD and DCS). To reduce the potential effect of cloud-induced low light conditions, we calculated the daily clearness index (Gu et al., 1999) and then excluded those cloudy days with a clearness index <0.3 (Zhang et al., 2011). Daily data of midday (10am ~ 2pm) mean GPP and diurnal metrics were averaged to monthly data, but any months with valid days of <10 were excluded. Monthly data were further averaged to produce annual data for each of the six years. The same temporal averaging scheme was applied to derive monthly and annual meteorological data using midday mean values, except rain using daily cumulative values. Pearson's correlation analyses were used to explore potential links among GPP, diurnal metrics, and meteorological variables.

To examine the response of GPP and diurnal metrics to the combination of heat and drought stresses, all valid days over the six-year study period were divided into 10 × 10 groups according to the percentiles of both T_{air} and VPD and then the mean value of those days within each group was calculated. The responses of RMD to heat or drought stress individually were further analyzed, where linear regressions were applied to the data of all years to quantify the overall sensitivity of daily and monthly RMD to each stress, i.e., the slope of the fitted line. Linear regressions between daily RMD and both stresses were also conducted for each single year, and then the response of these sensitivities to annual rain was further examined to reveal the long-term impact of rain on RMD.

3. Results

3.1. Temporal variations in GPP, diurnal metrics, and meteorological factors

The time series of monthly meteorological factors, GPP, and diurnal metrics, had strong seasonal variations over the six-year study period (Fig. 2a). Monthly midday T_{air} showed a clear seasonal pattern with higher (32.3 ± 0.4 °C; mean ± std.) and lower (19.4 ± 1.0 °C) values in summer and winter, respectively. The seasonal pattern of monthly midday VPD was similar to middy T_{air} with its seasonal peak in summer (1.34 ± 0.41 kPa). Rain most occurred in spring and summer with monthly rain up to 392.4 mm. Monthly midday GPP was higher in spring (18.2 ± 0.9 μmol m^{-2} s^{-1}) than other seasons (17.5 ± 1.3 μmol m^{-2} s^{-1}). Monthly RMD (−7.2 % ~ 26.1 %) varied seasonally with higher (16.1 ± 4.8 %) and lower (−2.7 ± 2.9 %) values in summer and winter, respectively, while no obvious seasonality of monthly DCS (−0.15 ± 0.07 h) was observed over the years.

Annual midday T_{air} increased from 26.7 °C in 2017 to 27.0 °C in 2018 and then decreased to 26.8 °C in 2021 and 2022 (Fig. 2b). Annual midday VPD had a linear increasing trend varying from 0.68 kPa in 2017 to 1.48 kPa in 2022. Annual rain varied from 1006.5 mm in 2020 to 1519.8 mm in 2022. Annual midday GPP changed over the years with the highest (18.9 μmol m^{-2} s^{-1}) and lowest (16.5 μmol m^{-2} s^{-1}) values in 2017 and 2021, respectively. Annual RMD changed from 5.0 % in 2017 to 10.2 % in 2020 with an inter-annual variation opposite to that of annual midday GPP (statistically significant at $p < 0.05$; Fig. 3b). Annual DCS was relatively stable varying from −0.17 h in 2018 to −0.12 h in 2022.

3.2. Environmental controls on GPP and diurnal metrics

Among the three investigated meteorological factors, monthly midday GPP was statistically significant correlated with VPD (correlation coefficient: −0.26), while its correlations with T_{air} (0.18) and rain (0.13) were not statistically significant (Fig. 3a). Monthly RMD was statistically significantly correlated with all the meteorological factors, with a stronger correlation with T_{air} (0.89) than VPD (0.67) and rain (0.46). The correlations between monthly DCS and meteorological factors were not statistically significant. At the annual scale, there was no statistically significant correlation between GPP, RMD, DCS, and the meteorological factors (Fig. 3b).

To better examine environmental controls on GPP and diurnal metrics, we analyzed the responses of midday GPP, frequency of the occurrence of midday depression (FMD), RMD, and DCS to gradient increases in midday T_{air} and VPD (Fig. 4). The responding patterns of GPP, FMD, and RMD were overall clearer than those of DCS. GPP increased with T_{air} but decreased with VPD, tending to have larger values when T_{air} and VPD were higher and lower than their medians, respectively. The magnitude of GPP increased from 14.5 μmol m^{-2} s^{-1} at low T_{air} and high VPD to 20.4 μmol m^{-2} s^{-1} at high T_{air} and low VPD. RMD increased with both T_{air} and VPD showing a tipping point around

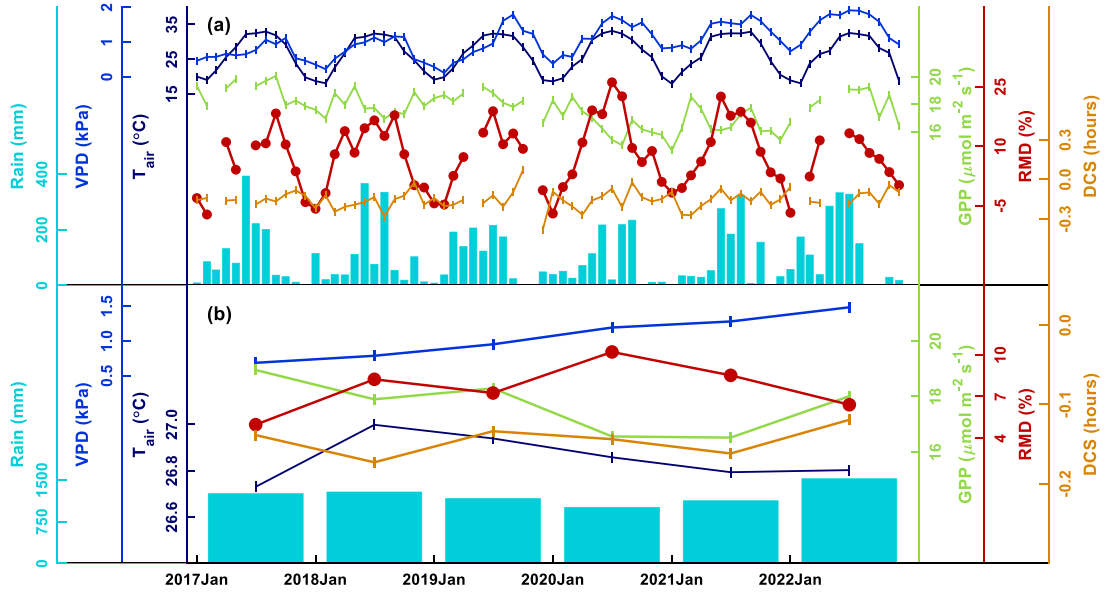

Fig. 2. Temporal variations of monthly (a) and annual (b) midday mean gross primary productivity (GPP), relative midday depression (RMD), diurnal centroid shift (DCS), as well as environmental factors, including midday mean air temperature (T_{air}), midday mean vapor pressure deficit (VPD), and rain, from January 2017 to December 2022. Data gaps in monthly variables denote the months with the number of valid days <10.

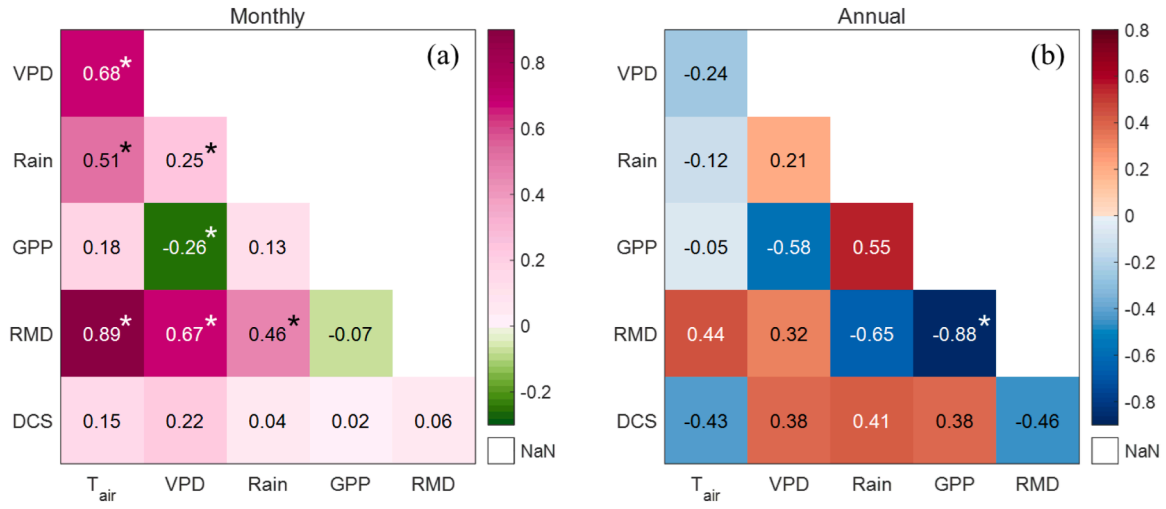

Fig. 3. Paired Pearson's correlation coefficients between (a) monthly and (b) annual midday mean gross primary productivity (GPP), relative midday depression (RMD), diurnal centroid shift (DCS), as well as environmental factors, including midday mean air temperature (T_{air}), midday mean vapor pressure deficit (VPD), and rain. Note that each statistically significant ($p < 0.05$) coefficient is marked with an asterisk.

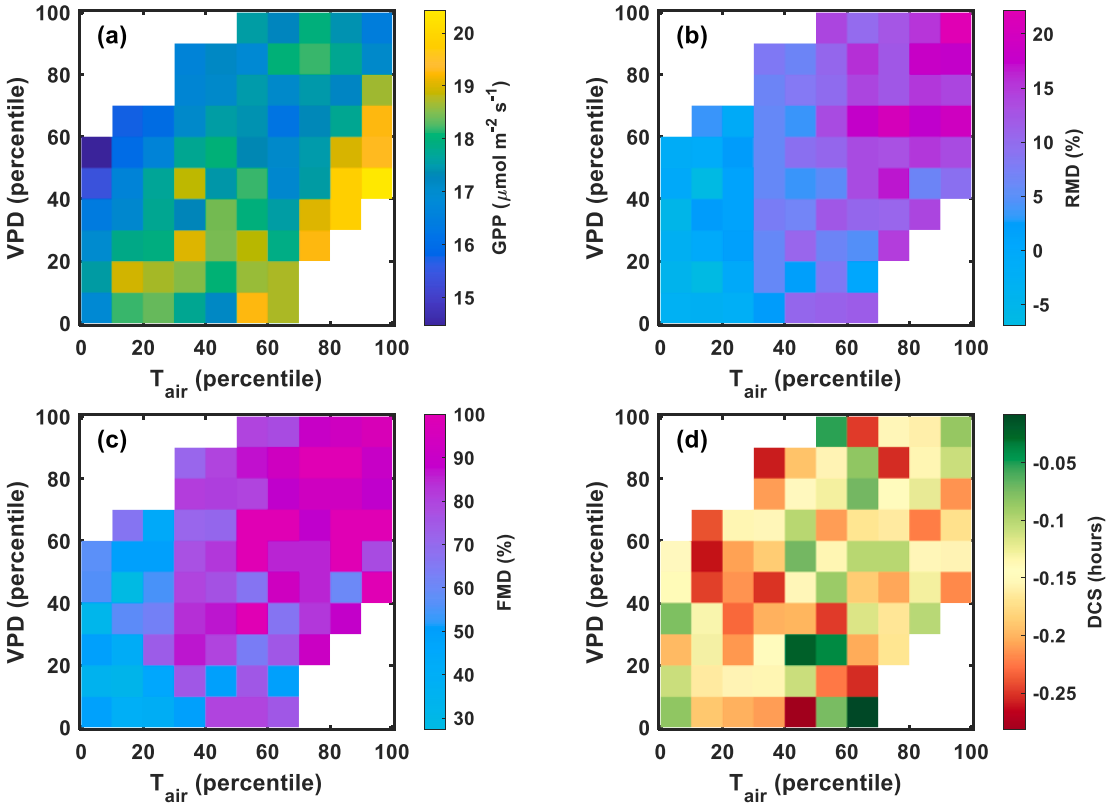

Fig. 4. Responses of midday mean gross primary productivity (GPP) (a), midday mean relative midday depression (RMD) (b), frequency of the occurrence of midday depression (FMD) (c), and diurnal centroid shift between GPP and photosynthetically active radiation (DCS) (d) to gradient increases in midday mean air temperature (T_{air}) and vapor pressure deficit (VPD). All days with valid data availability over the six-year study period are first divided into 10 × 10 groups (or grids) according to the percentiles of both T_{air} and VPD (see Tables S1-S3 for quantitative information on actual data) and then the mean/frequency values of those days within each group are shown for each grid. Any group with valid days not >5 days is excluded from the analyses (i.e., white grids). FMD is calculated as the percentage of positive RMD over all RMD within each group.

the median, beyond which the combination of high T_{air} and VPD led to stronger RMD up to 22.2 %. FMD also increased with both T_{air} and VPD with most of the values over 60 %. DCS was always negative (i.e., a morning shift relative to the centroid of diurnal PAR) varying from −0.28 h to −0.01 h.

Given that RMD can serve a direct metric to measure the down-regulation effect of MD on GPP, we further examined the quantitative response of RMD to individual heat or drought stress based on daily (binned) and monthly data over the six-year study period (Fig. 5). Both daily (binned) and monthly RMD were positively correlated to T_{air} with a larger fitted slope for monthly data (daily/binned: $y = 1.03x - 20.00$, $R^2 = 0.92$, $p < 0.05$; monthly: $y = 1.39x - 29.37$, $R^2 = 0.79$, $p < 0.05$).

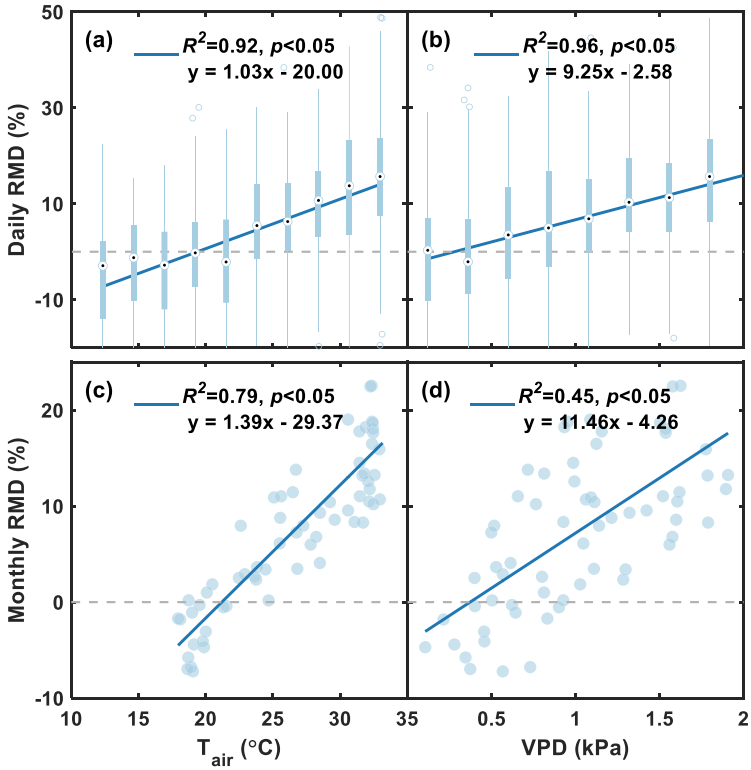

Fig. 5. Responses of daily (a and b) and monthly (c and d) relative midday depression (RMD) to midday mean air temperature (T_{air}) and vapor pressure deficit (VPD) as well as their linear regressions, based on the data over the six-year study period. For daily RMD, T_{air} or VPD is equally divided into ten groups, and then the mean RMD of each group is used for the linear regressions.

Similar relationships were found between RMD and VPD (daily/binned: $y = 9.25x - 2.58$, $R^2 = 0.96$, $p < 0.05$; monthly: $y = 11.46x - 4.26$, $R^2 = 0.45$, $p < 0.05$). According to the linear regressions, the fitted daily and monthly RMD changed from negative to positive values at a temperature threshold of 19.4 °C and 21.1 °C, respectively, while the fitted daily and monthly RMD were positive over a VPD threshold of 0.3 kPa and 0.4 kPa, respectively.

3.3. Annual change in the response of RMD to heat and drought stresses

Although positive correlations between RMD and T_{air} and between RMD and VPD were observed for each year from 2017 to 2022 (statistically significant at $p < 0.05$), their sensitivities (i.e., the fitted linear slopes) differed among the years for both T_{air} and VPD (Fig. 6). The highest sensitivities of RMD to T_{air} (S_T =1.35 %/ °C) and VPD (S_{VPD} = 13.79 %/kPa) occurred in the same year of 2020, while the lowest S_T (1.01 %/ °C) and S_{VPD} (8.41 %/kPa) occurred in 2017 and 2022, respectively. Correlation analyses between these two sensitivities and annual meteorological factors indicated that annual rain could explain 65 % and 74 % of the inter-annual variability of S_T and S_{VPD}, respectively (Fig. 7). Both annual S_T ($y = -0.73x + 2.06$, $R^2 = 0.65$, $p < 0.05$) and S_{VPD} ($y = -9.84x + 24.46$, $R^2 = 0.74$, $p < 0.05$) were negatively correlated with annual rain. According to the regressions, S_T and S_{VPD} would decrease from 1.33 %/ °C to 0.97 %/ °C and from 14.62 %/kPa to 9.70 %/kPa, respectively, when annual rain increased from 1000 mm to 1500 mm.

4. Discussion

The analyses of six-year EC and environmental measurements confirm the importance of heat and drought stresses, including T_{air}, VPD, and rain, in regulating the temporal variability of mangrove GPP and MD. Higher T_{air} and VPD and less rain, occurring in summer and early autumn, exert heat and drought stresses on this mangrove and result in lower GPP and higher RMD (Fig. 2a). This inhibitory effect on mangrove photosynthesis is also reported by previous studies, which mainly attribute the inhibition to enhanced VPD and reduced stomatal conductance (Leopold et al., 2016; Liu and Lai, 2019; Pathre et al., 1998). Our analyses support that mangrove MD is a common phenomenon occurring on sunny days in hot and dry months. Similar to Tüffers et al. (1999) reporting higher mangrove RMD in July than in November, monthly RMD in this mangrove is also higher in hotter and drier months for each year (Fig. 2a). The extent of daily RMD under hotter and drier conditions over the six years (Figs. 5a-b) is also within the varying range of previous studies (10 ~ 40 %) (Sobrado, 1999; Tüffers et al., 1999).

The correlation analyses confirm the links between RMD and the three meteorological factors at a monthly scale, with RMD being most coupled with T_{air} (Fig. 3a). This suggests that MD in this mangrove is strongly sensitive to heat and drought stresses. The weak coupling between DCS and meteorological factors (Figs. 3 and 4d) implies that DCS cannot serve as a good diurnal metric to quantify mangrove MD. The regression analyses suggest that daily/monthly RMD are positively correlated with both T_{air} and VPD (Fig. 5), which supports our first hypothesis that mangrove MD enhances with increasing heat and drought stresses. This is consistent with many previous studies reporting a downregulation of mangrove CO_2 uptake when experiencing high temperature and VPD (Alvarado-Barrientos et al., 2021; Liu and Lai, 2019; Rodda et al., 2022). The strengthened RMD at high T_{air} and VPD (Fig. 4b) suggests the combination of heat and drought stresses can exert a superposition effect on the downregulation of mangrove photosynthesis. This is in line with the finding that mangroves can even experience a mass dieback event when heat and drought stresses occur simultaneously (Duke et al., 2021). Rain poses a negative effect on RMD at an annual scale (Fig. 7b), while it is positively correlated with RMD at a monthly scale (Fig. 7a). This positive rain-RMD correlation is not abnormal because monthly rain covaries with Tair and VPD (Fig. 2a),

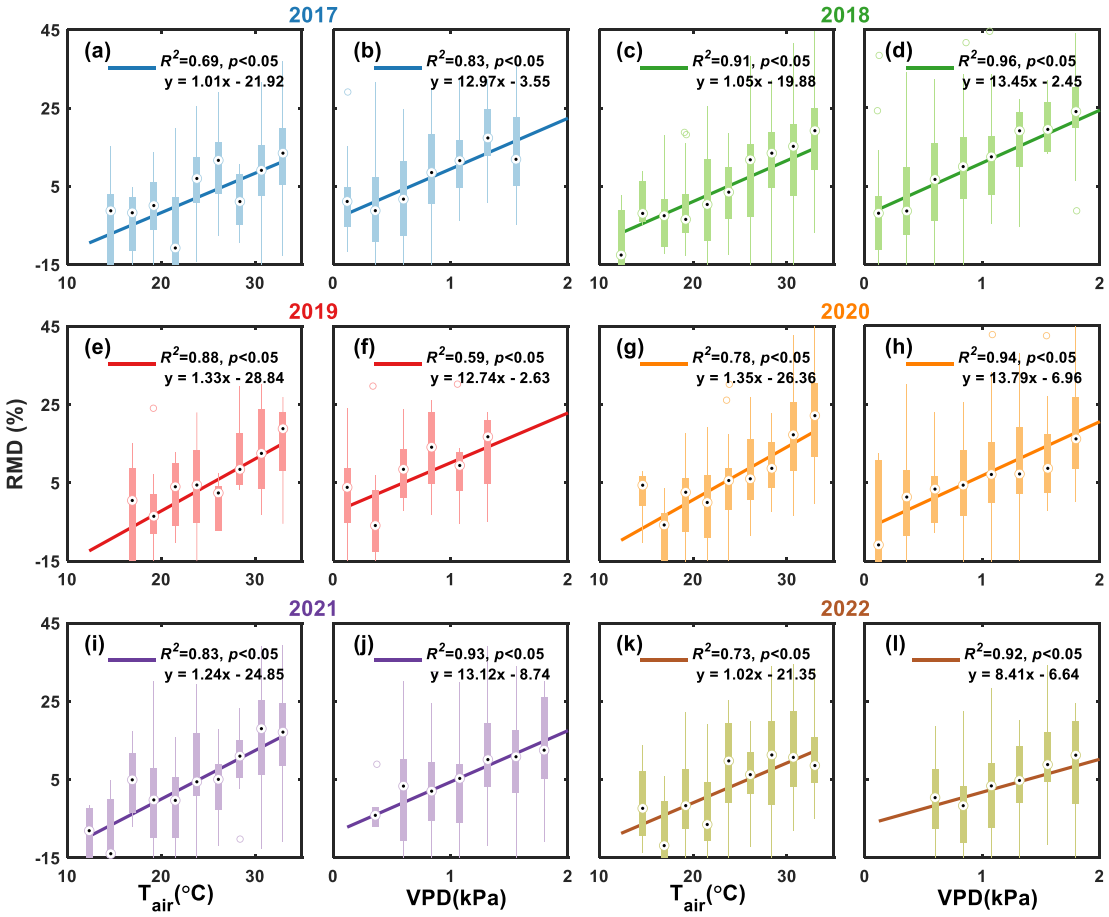

Fig. 6. Responses of daily relative midday depression (RMD) to midday mean air temperature (T_{air}) and vapor pressure deficit (VPD) as well as their linear regressions, based on the data in each year. T_{air} or VPD is grouped in equal differences based on the full data range of all years, and then the mean RMD of each group are used for the linear regressions.

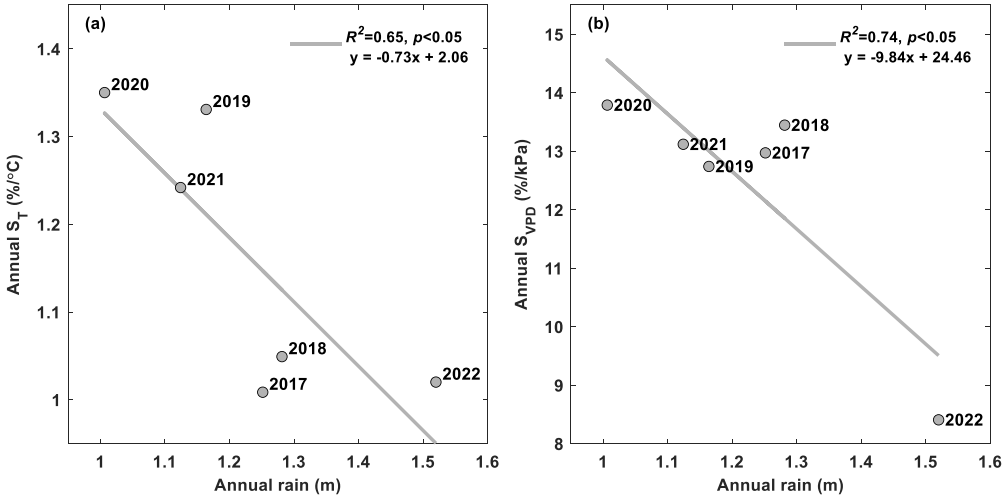

Fig. 7. Changes in the sensitivities (i.e., the slopes of fitted lines in Fig. 6) of relative midday depression to midday mean daytime air temperature (S_T; a) and vapor pressure deficit (S_{VPD}; b) as a function of annual rain over the six-year study period. Linear regressions are shown for the relationships.

which dominate the seasonality of monthly RMD.

The regression analyses also indicate larger fitting slopes (after normalization by the range of independent variables) in the T_{air}-RMD regression than those in the VPD-RMD regression (Fig. 5), which further confirms that mangrove MD is more driven by heat stress. The existence of T_{air} and VPD thresholds suggests that mangrove MD does not always occur until the stresses increase beyond the thresholds. Although RMD always enhances with increasing heat and drought stresses in each of the six years, annual responding sensitivity varies across years with stronger S_T and S_{VPD} corresponding to lower rain (Fig. 7). This finding supports our second hypothesis that the annual responding sensitivity of mangrove MD to heat and drought stresses reduces with more rain. In

other words, mangrove MD would be more sensitive to heat and drought stress if they experience less rain than usual. This rain-induced relief on mangrove MD coincides with our previous finding that drought-induced salinity enhancement weakens annual CO_2 uptake by this mangrove (Zhu et al., 2021c).

Our EC-based data analyses of mangrove MD suffer from several limitations and uncertainties. First, since GPP time series are derived from raw 10-Hz EC measurements, and thus the uncertainties in GPP and MD come from EC data processing procedures including flux corrections, quality controls, and flux partitioning (Reichstein et al., 2005). In particular, errors in GPP and MD could arise from flux partitioning from NEE into GPP and *Re* since increasing midday T_{air} leads to higher *Re* and lower NEE, which is not actually related to MD. As shown by the mean diurnal variations in 30-min NEE, GPP, *Re*, and their responses to environmental controls (Fig. S1), mangrove GPP does experience depression during midday hours after excluding the confounding effect of *Re*, which confirms the occurrence of mangrove MD with heat and drought stress. As shown by the diurnal variations in actual and fitted GPP under stress-free conditions (Fig. S2), we also confirm that the fittings of Eq. (2) well track the daytime course of GPP and thus RMD serves a good metric to quantify the severity of mangrove MD. Second, since the EC data represents spatially integrated signals over the footprint, the temporal variations of GPP across various time scales are also regulated by the time-varying footprint. Thus, our analyses only represent ecosystem-level MD rather than leaf- or plot-level MD targeted for specific mangrove species. Third, given that the dominant mangrove species within the EC footprint, *Kandelia obovata* and *Avicennia marina*, are more heat-sensitive (Li et al., 2022), the interactions between mangrove MD and environmental stresses revealed by this study might be species-dependent and thus any extrapolation to other species or climate region should be taken with cautions. Lastly, linear and synchronous processes are implicitly assumed in this study to explore the responses of mangrove MD to environmental stresses, however, carbon fluxes in wetland ecosystems often involve nonlinear and asynchronous processes across time scales (Sturtevant et al., 2016). Future studies using advanced statistical techniques combined with more available measurements are needed to assess this uncertainty (Knox et al., 2021).

5. Conclusion

Temporal variations in mangrove GPP and MD as well as their responses to heat (air temperature) and drought (VPD and rain) stresses across time scales are investigated in a subtropical estuarine wetland of Southeast China, based on six-year simultaneous measurements of EC and meteorological data from 2017 to 2022. We find that RMD serves a good metric to quantify the extent of mangrove MD that occurs with air temperature or VPD above a certain threshold and becomes severe when the stresses co-exist. Monthly RMD has a clear seasonal pattern peaking in summer, reflecting its seasonal controls of heat and drought stresses. Annual RMD changes in the opposite direction with GPP, indicating the contribution of MD to the reduction in GPP. The sensitivity of RMD to heat and drought stresses varies across years with stronger ones occurring in drier years with less rain. This study highlights the importance of heat and drought stresses in affecting mangrove MD and GPP, implying that future warmer and drier climates are likely to weaken mangrove carbon uptake. The findings on the interactions between mangrove MD and environmental stresses across time scales provide direct empirical evidence for a better understanding of the response of mangrove blue carbon to climate change. To reduce the uncertainty in assessing mangrove carbon budget in the context of climate change, future empirical and model studies on mangrove blue carbon should explicitly consider the sub-daily interactions that are likely obscured when interpreting the seasonal or annual variability using aggregating daily or multi-day observations.

CRediT authorship contribution statement

Zhu Zhu: Writing – original draft, Visualization, Validation, Methodology, Investigation, Formal analysis, Data curation. **Xudong Zhu:** Writing – review & editing, Visualization, Validation, Supervision, Resources, Project administration, Methodology, Investigation, Funding acquisition, Formal analysis, Data curation, Conceptualization.

Declaration of competing interest

The authors declare that they have no known competing financial interests or personal relationships that could have appeared to influence the work reported in this paper.

Acknowledgments

We are grateful to the staff at Zhangjiang Estuary Mangrove National Nature Reserve for their help in the fieldwork. This work was jointly supported by the National Natural Science Foundation of China (32371661), the Natural Science Foundation of Fujian Province of China (2023J06008), the National Key Research and Development Program of China (2022YFF0802101), Shenzhen Science and Technology Plan Project (KCXST20221021111404011), the Open Fund of Fujian Key Laboratory of Severe Weather (2022KFKT03), and the 2023 Google Carbon Removal Research Awards.

Data availability

Data will be made available on request.

References

Alongi, D.M., 2014. Carbon cycling and storage in mangrove forests. Ann. Rev. Mar. Sci. 6 (1), 195–219.
Alongi, D.M., Mukhopadhyay, S.K., 2015. Contribution of mangroves to coastal carbon cycling in low latitude seas. Agric. For. Meteorol. 213, 266–272.
Alvarado-Barrientos, M., Lopez-Adame, H., Lazcano-Hernandez, H.E., Arellano-Verdejo, J., Hernandez-Arana, H.A., 2021. Ecosystem-atmosphere exchange of CO_2, water, and energy in a basin mangrove of the northeastern coast of the Yucatan Peninsula. J. Geophys. Res. 126 (2), e2020JG005811.
Baldocchi, D., et al., 2001. FLUXNET: a new tool to study the temporal and spatial variability of ecosystem-scale carbon dioxide, water vapor, and energy flux densities. Bull. Amer. Meteorol. Soc. 82 (11), 2415–2434.
Barr, J.G., Engel, V., Fuentes, J.D., Fuller, D.O., Kwon, H., 2013. Modeling light use efficiency in a subtropical mangrove forest equipped with CO_2 eddy covariance. Biogeosciences. 10 (3), 2145–2158.
Barr, J.G., Engel, V., Fuentes, J.D., Zieman, J.C., O'Halloran, T.L., Smith III, T.J., Anderson, G.H., 2010. Controls on mangrove forest-atmosphere carbon dioxide exchanges in western Everglades National Park. J. Geophys. Res. 115, G02020.
Chen, J.H., et al., 2023. Potential effects of sea level rise on the soil-atmosphere greenhouse gas emissions in *Kandelia obovata* mangrove forests. Acta Oceanologica Sinica 42 (4), 25–32.
Chung, C.T.Y., Hope, P., Hutley, L.B., Brown, J., Duke, N.C., 2023. Future climate change will increase risk to mangrove health in Northern Australia. Commun. Earth. Environ. 4, 193.
Duke, N.C., Hutley, L.B., Mackenzie, J.R., Burrows, D., 2021. Processes and factors driving change in mangrove forests: an evaluation based on the mass dieback event in Australia's Gulf of carpentaria. In: Canadell, J.G., Jackson, R.B. (Eds.), Ecosystem Collapse and Climate Change. Springer International Publishing, Cham, pp. 221–264.
Duke, N.C., et al., 2017. Large-scale dieback of mangroves in Australia's Gulf of Carpentaria: a severe ecosystem response, coincidental with an unusually extreme weather event. Mar. Freshwater Res. 68 (10), 1816–1829.
Gou, R., et al., 2023. Temporal variations of carbon and water fluxes in a subtropical mangrove forest: insights from a decade-long eddy covariance measurement. Agric. For. Meteorol. 343, 109764.
Gu, L., Fuentes, J., Shugart, H., Staebler, R., Black, T., 1999. Responses of net ecosystem exchanges of carbon dioxide to changes in cloudiness: results from two North American deciduous forests. J. Geophys. Res. 104, 31421–31434.
Knox, S.H., et al., 2021. Identifying dominant environmental predictors of freshwater wetland methane fluxes across diurnal to seasonal time scales. Glob. Chang. Biol. 27 (15), 3582–3604.
Leopold, A., et al., 2016. Net ecosystem CO_2 exchange in the "Coeur de Voh" mangrove, New Caledonia: effects of water stress on mangrove productivity in a semi-arid climate. Agricult. Forest Meteorol. 223, 217–232.

Li, X., et al., 2023. New-generation geostationary satellite reveals widespread midday depression in dryland photosynthesis during 2020 western U.S. heatwave. Sci. Adv. 9 (31), eadi0775.
Li, X., et al., 2022. Correlations between photosynthetic heat tolerance and leaf anatomy and climatic niche in Asian mangrove trees. Plant Biol. 24 (6), 960–966.
Liu, J., Lai, D.Y.F., 2019. Subtropical mangrove wetland is a stronger carbon dioxide sink in the dry than wet seasons. Agricultural and Forest Meteorology, 278, p. 107644.
Lovelock, C.E., Krauss, K.W., Osland, M.J., Reef, R., Ball, M.C., 2016. The physiology of mangrove trees with changing climate. In: Goldstein, G., Santiago, L.S. (Eds.), Tropical tree physiology: adaptations and responses in a changing environment. Springer International Publishing, Cham, pp. 149–179.
Lu, Y., Zhu, X., 2021. Response of mangrove carbon fluxes to drought stress detected by photochemical reflectance index. Remote Sens. 13 (20).
Macreadie, P.I., Costa, M.D.P., Atwood, T.B., Friess, D.A., Kelleway, J.J., Kennedy, H., Lovelock, C.E., Serrano, O., Duarte, C.M., 2021. Blue carbon as a natural climate solution. Nature Rev. Earth Environ. 2, 826–839.
Myhre, G., et al., 2019. Frequency of extreme precipitation increases extensively with event rareness under global warming. Sci. Rep. 9 (1), 16063.
Nellemann, C., Corcoran, E., 2009. Blue carbon: the role of healthy oceans in binding carbon. A rapid response assessment. UNEP/Earthprint.
Nelson, J.A., Carvalhais, N., Migliavacca, M., Reichstein, M., Jung, M., 2018. Water-stress-induced breakdown of carbon–water relations: indicators from diurnal FLUXNET patterns. Biogeosciences. 15 (8), 2433–2447.
Pathre, U., Sinha, A.K., Shirke, P.A., Sane, P.V., 1998. Factors determining the midday depression of photosynthesis in trees under monsoon climate. Trees-Struct. Funct. 12 (8), 472–481.
Perri, S., Detto, M., Porporato, A., Molini, A., 2023. Salinity-induced limits to mangrove canopy height. Global Ecol. Biogeogr. 32 (9), 1561–1574.
Pons, T.L., Welschen, R.A.M., 2003. Midday depression of net photosynthesis in the tropical rainforest tree *Eperua grandiflora*: contributions of stomatal and internal conductances, respiration and Rubisco functioning. Tree Physiol. 23 (14), 937–947.
Prihantono, J., Nakamura, T., Nadaoka, K., Wirasatriya, A., Adi, N.S., 2022. Rainfall variability and tidal inundation influences on mangrove greenness in Karimunjawa National Park, Indonesia. Sustainability 14 (14), 8948.
Reichstein, M., et al., 2005. On the separation of net ecosystem exchange into assimilation and ecosystem respiration: review and improved algorithm. Glob. Chang. Biol. 11 (9), 1424–1439.
Rodda, S.R., Thumaty, K.C., Fararoda, R., Jha, C.S., Dadhwal, V.K., 2022. Unique characteristics of ecosystem CO_2 exchange in sundarban mangrove forest and their relationship with environmental factors. Estuar. Coast Shelf S. 267, 107764.
Sharma, S., et al., 2020. The impacts of degradation, deforestation and restoration on mangrove ecosystem carbon stocks across Cambodia. Sci. Total Environ. 706, 135416.
Simard, M., et al., 2019. Mangrove canopy height globally related to precipitation, temperature and cyclone frequency. Nat. Geosci. 12 (1), 40–45.
Sobrado, M.A., 1999. Drought effects on photosynthesis of the mangrove, *Avicennia germinans*, under contrasting salinities. Trees-Struct. Funct. 13 (3), 125–130.
Sturtevant, C., et al., 2016. Identifying scale-emergent, nonlinear, asynchronous processes of wetland methane exchange. J. Geophys. Res. 121 (1), 188–204.
Tüffers, A.V., Naidoo, G., von Willert, D.J., 1999. The contribution of leaf angle to photoprotection in the mangroves *Avicennia marina* (Forssk.) Vierh. and *Bruguiera gymnorrhiza* (L.) Lam. under field conditions in South Africa. Flora 194 (3), 267–275.
Wang, C., et al., 2023. Variations in CO_2 and CH_4 exchange in response to multiple biophysical factors from a mangrove wetland park in southeastern China. Atmosphere 14 (5), 805.
Wilson, K.B., et al., 2003. Diurnal centroid of ecosystem energy and carbon fluxes at FLUXNET sites. J. Geophys. Res. 108 (D21).
Xia, P., et al., 2015. Mangrove development and its response to environmental change in Yingluo Bay (SW China) during the last 150 years: stable carbon isotopes and mangrove pollen. Org. Geochem. 85, 32–41.
Xiao, J., Fisher, J.B., Hashimoto, H., Ichii, K., Parazoo, N.C., 2021. Emerging satellite observations for diurnal cycling of ecosystem processes. Nat. Plants. 7 (7), 877–887.
Xu, D.Q., Shen, Y.K., 1996. Midday depression of photosynthesis. Handbook Photosynth 451–459.
Yuan, W., et al., 2019. Increased atmospheric vapor pressure deficit reduces global vegetation growth. Sci. Adv. 5 (8), eaax1396.
Zani, D., Crowther, T.W., Mo, L., Renner, S.S., Zohner, C.M., 2020. Increased growing-season productivity drives earlier autumn leaf senescence in temperate trees. Science 370 (6520), 1066–1071.
Zhang, M., et al., 2011. Effects of cloudiness change on net ecosystem exchange, light use efficiency, and water use efficiency in typical ecosystems of China. Agric. For. Meteorol. 151 (7), 803–816.
Zhang, Y., et al., 2018. On the relationship between sub-daily instantaneous and daily total gross primary production: implications for interpreting satellite-based SIF retrievals. Remote Sens. Environ. 205, 276–289.
Zhu, X., Hou, Y., Weng, Q., Chen, L., 2019. Integrating UAV optical imagery and LiDAR data for assessing the spatial relationship between mangrove and inundation across a subtropical estuarine wetland. ISPRS J. Photogramm. Remote Sens. 149, 146–156.
Zhu, X., et al., 2021a. Potential of sun-induced chlorophyll fluorescence for indicating mangrove canopy photosynthesis. J. Geophys. Res. 126 (4) e2020JG006159.
Zhu, X., Qin, Z., Song, L., 2021b. How land-sea interaction of tidal and sea breeze activity affect mangrove net ecosystem exchange? J. Geophys. Res. Atmosph. 126 (8) e2020JD034047.
Zhu, X., Sun, C., Qin, Z., 2021c. Drought-induced salinity enhancement weakens mangrove greenhouse gas cycling. J. Geophys. Res. 126 (8) e2021JG006416.
Zhu, X., et al., 2021d. Potential of sun-induced chlorophyll fluorescence for indicating mangrove canopy photosynthesis. J. Geophys. Res. 126 (4).